LA-UR -92-3417

LA-UR--92-3417

DE93 003723

Los Alamos National Laboratory is operated by the University of California for the United States Department of Energy under contract W-7405-ENG-36

TITLE USE OF THE NUCLEAR MODEL CODE GNASH TO CALCULATE CROSS SECTION DATA AT ENERGIES UP TO 100 MeV

AUTHOR(S) P. G. Young, M. B. Chadwick, and M. Bozoian
Group T-2, LANL

SUBMITTED TO The SYMPOSIUM ON NUCLEAR DATA EVALUATION METHODOLOGY
Brookhaven National Laboratory, Upton, NY
12-16 October 1992

DISCLAIMER

Los Alamos Los Alamos National Laboratory
Los Alamos, New Mexico 87545

USE OF THE NUCLEAR MODEL CODE GNASH TO CALCULATE CROSS SECTION DATA AT ENERGIES UP TO 100 MEV

P. G. YOUNG, M. B. CHADWICK, and M. BOZOIAN
Group T-2, Theoretical Division, Los Alamos National Laboratory
Los Alamos, NM 87545, USA

ABSTRACT

The nuclear theory code GNASH has been used to calculate nuclear data for incident neutrons, protons, and deuterons at energies up to 100 MeV. Several nuclear models and theories are important in the 10 - 100 MeV energy range, including Hauser-Feshbach statistical theory, spherical and deformed optical models, preequilibrium theory, nuclear level densities, fission theory, and direct reaction theory. In this paper we summarize general features of the models in GNASH and describe the methodology utilized to determine relevant model parameters. We illustrate the significance of several of the models and include comparisons with experimental data for certain target materials that are important in applications.

1. Introduction

The first version of the GNASH nuclear theory code was completed in 1974,[1] and it has been developed continually since that time. Several versions of the code are in use, including one adapted for use in generating activation cross sections for the Japanese fusion program,[2] and two versions with modifications and approximations suitable mainly for higher energy calculations.[3] The code discussed here is the base version and has been used for calculations at energies as low as 1 keV and as high as 100 MeV. It is best summarized as the statistical Hauser-Feshbach plus preequilibrium version with full angular momentum conservation.[4]

GNASH has been used to support many data evaluations at incident energies below 20 MeV, including several of the ENDF/B-VI evaluations. In recent years the code has been extended for work at higher energies and has been utilized in evaluations up to incident energies of 100 MeV. In particular, it was used for comprehensive analyses of neutron-induced reactions to 40 MeV for ^{56}Fe,[5] to 50 MeV for ^{59}Co,[6] and to 100 MeV with initial calculations for ^{208}Pb.[7] Additionally, a set of neutron- and proton-induced transport data libraries were generated with GNASH to an incident energy of 100 MeV for ^{27}Al, ^{28}Si, ^{56}Fe, ^{184}W, and ^{238}U,[8] and similar libraries are presently under development for deuteron-induced reactions to 100 MeV on ^{27}Al and ^{208}Pb.

In this paper we summarize the methods and procedures used in performing calculations with GNASH in the energy range of 10 - 100 MeV. Because the basic methodology is to utilize physically meaningful nuclear model parameters that result in reasonable descriptions of experimental data, we summarize in Sec. 2 the major models that are used in GNASH. In Sec. 3 we describe some aspects of choosing model parameters for higher energies and we illustrate features of the nuclear models by comparing calculations with experimental data. Finally, Sec. 4 includes some conclusions and summary remarks concerning the use of GNASH at higher energies.

2. Nuclear Models Used in GNASH

A block diagram summarizing the various input and output quantities for a GNASH calculation is included as Fig. 1. The input information includes separate files of discrete level decay data for all significant residual nuclei that are formed in a given problem, optical model transmission coefficients, direct reaction cross sections, and ground-state mass, spin and parity tables. The remaining model parameters, reaction sequences, calculational energy range, etc., are provided in an INPUT file.

GNASH implements Hauser-Feshbach theory in an open-ended sequence of reaction chains, with full conservation of angular momentum. Reaction chains are defined in the code input, either by direct specification of the sequence or by setting a flag to indicate a particular decay chain option. A schematic illustration of the decay processes that occur for each compound nucleus in a decay sequence is given in Fig. 2. Note in the simplified expressions at the bottom of the figure that the change in population of states in the residual nucleus (K') from transitions from the initial (K) nucleus is proportional to the transmission coefficient, $T(U\text{-}U'\text{-}B')$, for the radiation and to the level density, $\rho(U')$, of the final nucleus. Transmission coefficients for particles are obtained from optical model calculations and for gamma rays from a giant dipole resonance model. In addition to being important for providing transmission coefficients, optical model potentials are used to obtain the initial compound nucleus formation cross section, which then determines the overall normalization of all calculated emission cross sections. Continuum level densities are obtained from phenomenological level density functions,[9,10] which are matched at lower excitation energies to the available discrete level data. Both the discrete and continuum structure data are utilized in GNASH calculations.

Preequilibrium corrections become increasingly important at energies above 20 MeV and are made in GNASH using the exciton model of Kalbach.[11] We demonstrate below that for certain applications it is also important to include multiple preequilibrium effects for secondary neutrons and protons as well as the usual corrections in the primary decay channels. Width fluctuation corrections can be applied to decays from the initial compound nucleus, although these are not important for the energy range discussed here. For actinide studies, the code contains a detailed fission model, allowing use of up to three uncoupled fission barriers. The models are expected to be applicable over a wide energy range, and GNASH has been utilized from incident energies below 1 keV to above 100 MeV.

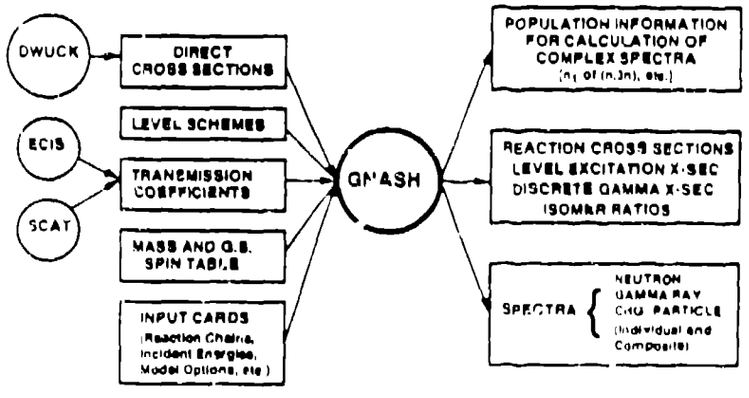

Fig. 1. Schematic representation of the input and output capabilities of the GNASH code.

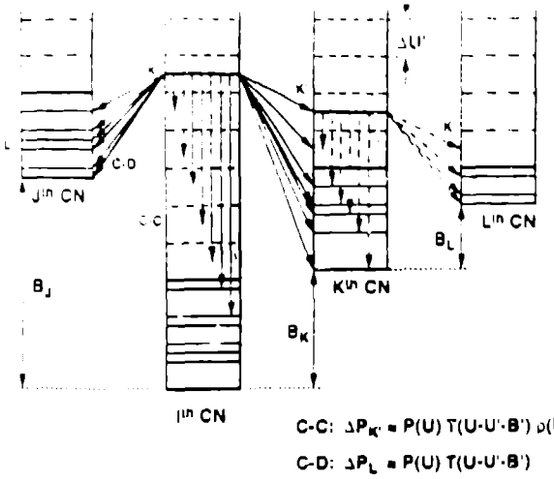

Fig. 2. Illustration of the decay of a continuum energy bin in the I^{th} compound nucleus to continuum (C - C) and discrete (C - D) states in the J^{th} and K^{th} compound systems. Simplified equations depicting the continuum to continuum and continuum to discrete population increments are given.

Referring to Fig. 1, the primary output from GNASH are absolute angle-integrated particle and gamma-ray spectra, and excitation and deexcitation cross sections of discrete states. The calculated spectra are integrated and summed to provide absolute reaction cross sections. The present configuration of the code permits the incident particle type to be neutrons, protons, deuterons, tritons, ^{3}He, or ^{4}He. In addition to gamma rays, these same particles are permitted in the decay channels. Angular effects are not included in the calculations, as the results are normally used in combination with the systematics-based parameterization of Kalbach[12] to determine angular distributions. For this purpose, the code provides tables of ratios of preequilibrium to total emission cross sections as functions of emission energy for all outgoing particles, as required in applying the Kalbach relations.

3. Calculational Method and Parameter Selection for the Nuclear Models

The methodology followed in performing GNASH calculations at higher energies varies from problem to problem and clearly depends on the end use of the results. For example, several of the libraries we have developed are mainly for radiation transport calculations and only contain total emission spectra for secondary particles and gamma rays, without specification of the cross sections for individual reactions or discrete level transitions.[8] On the other hand, we are also involved in analyzing results from measurements in very detailed experiments where individual gamma rays from (n,xγ) reactions (x= 1-10) are measured.[7] In particular, we have used the GNASH code to calculate cross sections for all significant neutron-induced γ-ray producing reactions on ^{208}Pb up to E_n = 100 MeV. Demands on the modeling are obviously much more stringent in this case, and careful determination of certain model parameters is essential.

A typical sequence of operations in the course of calculations might include the following: (1) compile level structure data for all residual nuclei in a calculation; (2) obtain optical model potentials for all the particles of interest in a calculation and verify their validity over the energy range of interest; (3) compile data on direct reactions that might be of interest for an analysis; (4) verify level density, γ-ray strength function, preequilibrium, and fission model parameters to be used by calculating the available experimental data; (5) verify by sample calculations that all important decay channels are included in the problem. Elaboration of some of these steps with examples is given below. In particular, we compare the effects of different model or parameter choices in calculations of different reactions, with emphasis on ^{208}Pb(n,nxγ) cross sections for specific γ-rays.

3.1 *Optical Potentials*

There are a large number of global optical model potentials available for incident nucleons, and these are frequently used in GNASH calculations where accuracy requirements are only modest. However, a basic problem exists in carrying analyses to energies of 100 MeV or higher, because transmission coefficients are required in the Hauser-Feshbach calculations to low particle energies and global potentials usually do not cover such a large energy range. One method of handling this problem is to combine two potentials that span the energy region of the calculation, with particular attention to selecting a matching energy where the reaction cross sections from the two potentials are consistent. We have frequently combined the Madland[13] higher energy potential for protons and deuterons with one of the common lower energy potentials.[14]

Best results are usually obtained if analyses have been performed leading to potentials for the specific target nucleus and energy range under investigation. We are currently using GNASH to analyze high-resolution neutron-induced gamma-ray production measurements on Pb isotopes from the WNR/PSR facility at LAMPF, and three of the potentials we are studying are compared to neutron total cross section measurements[15] on ^{208}Pb in Fig. 3. Of the three optical model curves shown, only the Schutt et al.[16] analysis was directed specifically at n + ^{208}Pb data over the entire energy range shown. In particular, the Schutt et al.[16] potential results from an analysis of n + ^{208}Pb elastic scattering data to 40 MeV and total cross section data between 2 and 250 MeV. The Finlay et al.[17] potential results from an analysis of similar data between 7 and 50 MeV. For the calculation in Fig. 3, the Finlay potential was utilized to about 60 MeV and the Madland potential[13] at higher energies. The coupled-channel potential is a simple extrapolation of the low-energy Young and Shamu potential described at this symposium[18] that reasonably reproduces differential elastic scattering data near 20, 30, and 40 MeV. All three potentials agree with the measurement to within ≈ 2% at energies below 60 MeV, but the coupled-channel and Madland potentials lie ≈5-7% below the data in the 70-100 MeV range.

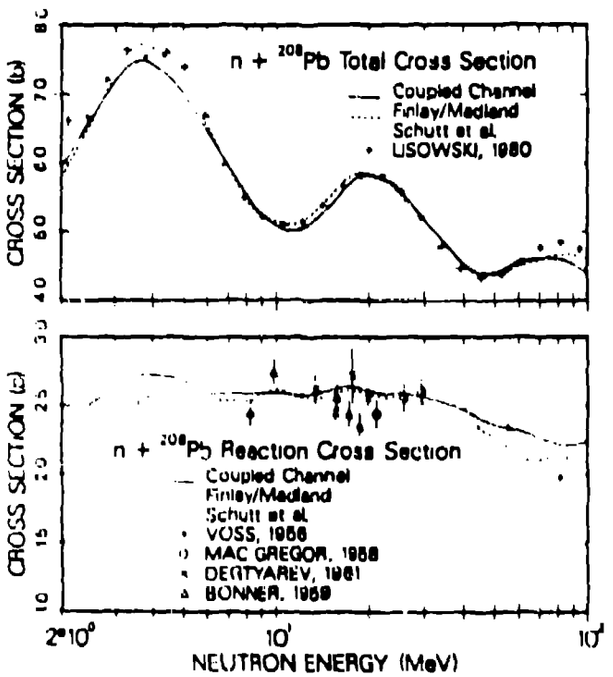

Fig. 3. Total and reaction cross sections for n + ^{208}Pb reactions between 2 and 100 MeV.

Results from the n + ^{208}Pb calculations using the above three optical potentials are compared in Fig. 4 to experimental results from Vonach et al.[19] The two cases shown are for the 570-keV gamma ray from the ^{208}Pb(n,2nγ)^{207}Pb reaction, corresponding to the transition from the 5/2$^-$ first excited state to the 1/2$^-$ ground state, and for the 803-keV gamma ray from the ^{208}Pb(n,3nγ)^{206}Pb reaction (2$^+$ first excited state to the 0$^+$ ground state). A standard set of models and parameters was used in the calculations, including the level density representation by Ignatyuk et al.[10] and default preequilibrium and giant dipole resonance parameters. None of the optical model choices results in calculated (n,xγ) cross sections that agree perfectly with the data over the entire energy range, but the calculations with the coupled-channel potential appears to represent the data best.

In extending GNASH calculations from the typical ENDF/B energy limit of 20 MeV to a range of 100 MeV, it is preferable to utilize relativistic kinematics in the supporting optical model calculations. In addition, care must be taken in the calculations to ensure that appropriate angular momentum is permitted in the optical model transmission coefficients provided to GNASH. This latter effect is illustrated in Fig. 4, where the results of GNASH calculations of d + ^{208}Pb reactions to 98 MeV using l_{max} = 20 and l_{max} = 32 are compared, with the latter limit being appropriate for this energy. The results shown are neutron emission spectra at 30^o and 105^o from a Pb stopping target and are compared to the measurements of Martin et al.[20] It might be noted that, while the validity of the Kalbach angular distribution systematics[12] have been thoroughly verified for incoming and outgoing nucleons, the results in Fig. 4 confirm their applicability over this angular range for incident deuterons and emission neutrons.

3.2 *Level Densities*

The GNASH code presently includes three options for phenomenological level densities: the Gilbert and Cameron model,[9] the back-shifted Fermi gas model,[21] and a form of Fermi gas model by Ignatyuk et al.[10] that includes an energy-dependent level density parameter and the damping out of shell effects at higher excitation energies. The Ignatyuk model is in better agreement with microscopic Fermi gas models, and its more realistic treatment of shell effects is especially important at higher excitation energies for calculations on target nuclei such as ^{208}Pb that lie at or near shell closures. The computed level density of ^{208}Pb using the Gilbert and Cameron formulation and that of Ignatyuk et al. differ at excitation energies above 50 MeV by many orders of magnitude.[8]

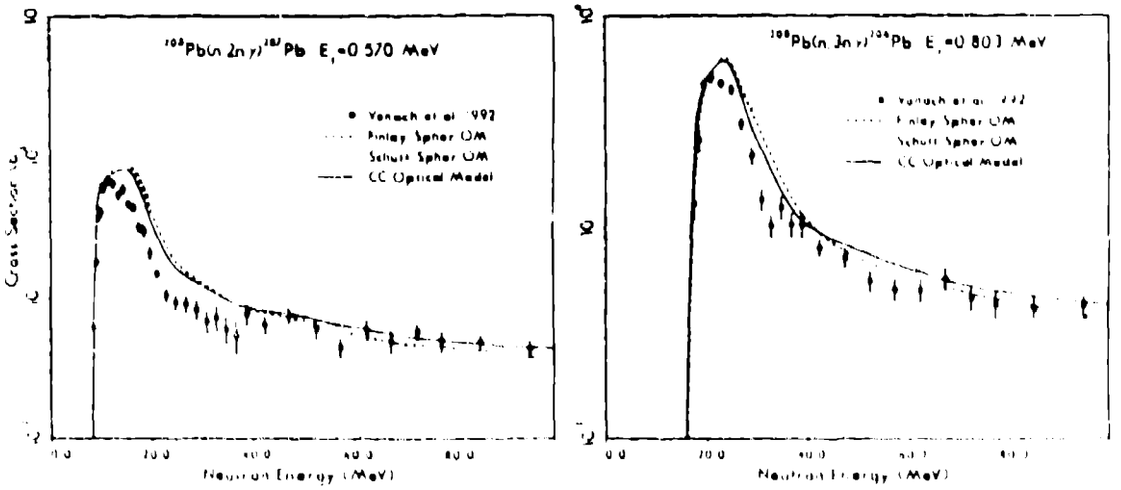

Fig. 4 Comparison of ^{208}Pb(n,2nγ)^{207}Pb and ^{208}Pb(n,3nγ)^{206}Pb cross sections calculated with transmission coefficients from three different optical model potentials with the data of Vonach et al.[10]

The results of GNASH calculations of $^{208}Pb(n,xn\gamma)$ cross sections using the Gilbert-Cameron and Ignatyuk formulations are compared in Fig. 6 with the measurements of Vonach et al.[19] The cases shown are for the 570-keV gamma ray from the $^{208}Pb(,2n\gamma)$ reaction, similar to Fig. 4, and the 961-keV gamma ray from the $^{208}Pb(n,7n\gamma)$ reaction from the 2^+ first excited state to the ground state of ^{202}Pb. The main effect of using the Gilbert and Cameron model is to successively shift the shape of $(n,xn\gamma)$ reactions to higher energies, with the effect becoming larger with increasing x. The Ignatyuk formulation clearly agrees better with the experimental data.

For nuclei more removed from shell closures, the effect seen in Fig 6 is much less pronounced. In Fig. 7 is shown a calculation of the $^{56}Fe(n,2n\gamma)^{55}Fe$ cross section for the 931-keV gamma ray, together with the measurements of Larson.[21] The calculations with both the Gilbert-Cameron and Ignatyuk level density models result in essentially equivalent agreement with the experimental data in Fig. 7.

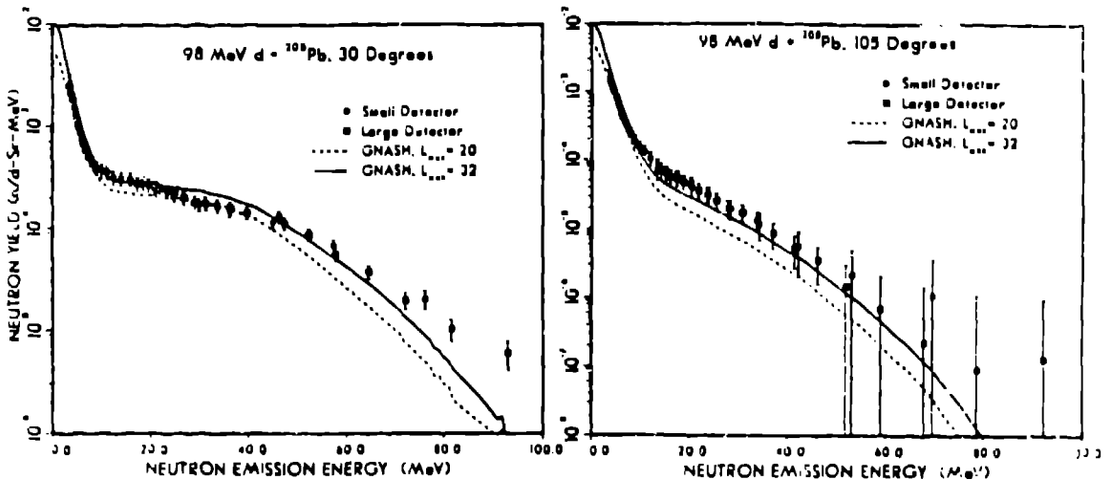

Fig. 5. Neutron emission spectra calculated with two different angular momentum cutoffs from a stopping Pb target bombarded with 98 MeV deuterons at 30° and 105°. The measurements are from Maruta et al.[20]

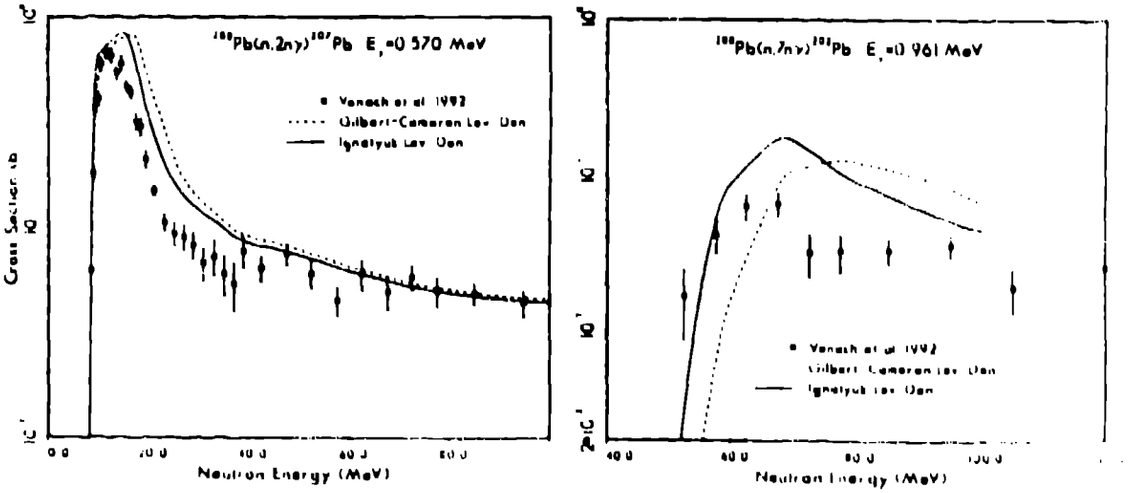

Fig. 6. Comparison of $^{208}Pb(n,2n\gamma)^{207}Pb$ and $^{208}Pb(n,7n\gamma)^{202}Pb$ cross sections calculated with two level density models[9,10] with the data of Vonach et al.[10]

3.3 *Preequilibrium and Direct Reactions*

The importance of preequilibrium processes at higher incident energies is well established. Preequilibrium reactions are pictured as successive excitation of particle-hole pairs in nucleon-nucleon collisions, distributing the incident energy among particle-hole pairs until equilibration is reached. The particles emitted in the early (simple) configurations typically contribute to the high-energy part of the emission spectra. Many preequilibrium calculations assume that at most only one nucleon is emitted from a preequilibrium stage. In this case preequilibrium nucleon emission would come from the dominant *2p1h* stage, and the residual *1p1h* nucleus is assumed to proceed to equilibrium via a series of nucleon-nucleon collisions. Composite reactions such as total particle emission are not drastically altered by the addition of multiple preequilibrium emission processes, even at neutron energies as high as 90 MeV.[8] The situation is quite different, however, for certain tertiary reactions such as (n,2nγ) and (n,3nγ) reactions, because the high energy component of second neutron emission tends to directly populate lower lying discrete states that produce gamma rays. This effect is illustrated in Fig. 8 by comparing GNASH calculations with and without multiple preequilibrium reactions for the 570-keV and 803-keV gamma rays from ^{208}Pb(n,2nγ)^{207}Pb and ^{208}Pb(n,3nγ)^{206}Pb reactions, respectively. Again, the calculations are compared to the measurements of Vonach et al.[19] Inclusion of multiple preequilibrium effects is seen to be essential for reproducing the energy dependence of the cross sections at higher energies.

The need to include direct reactions in evaluations of neutron or proton induced reactions is well known. In those cases, direct components are usually calculated in distorted wave Born approximation codes such as DWUCK, or in coupled-channel codes like ECIS. If one is concerned with calculating neutron or proton emission spectra from deuteron-induced reactions, direct reactions must also be taken into account at higher energies. In calculations with GNASH, we utilize the simple model of Serber[22] coupled with experimental information on total (d,n) or (d,p) cross sections to incorporate these direct effects. This method was used in the calculations of neutron emission from 98-MeV deuteron reactions with ^{208}Pb shown in Fig. 5, which agree well with stopping target measurements. The extent of the Serber contribution is shown in the angle-integrated neutron emission spectrum of Fig. 9 for 60-MeV deuterons on ^{208}Pb. The contribution is a maximum near 1/2 of the incident deuteron energy and increases the cross section at emission energies above ≈ 15 MeV by a factor of 2 or more.

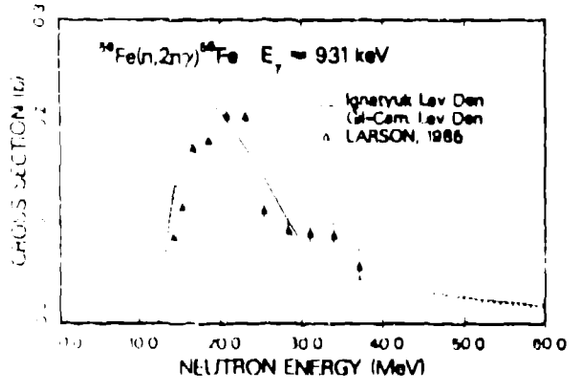

Fig. 7. Comparison of calculated and measured[21] values of the ^{56}Fe(n,2nγ)^{55}Fe cross section for the 0.931-MeV gamma ray with the Gilbert and Cameron[9] and Ignatyuk et al.[10] level density models.

4. Conclusions

The use of different models and parameter choices in calculations with the GNASH code confirms the importance of good optical model potentials and level density models that include reasonable representations of shell effects. The importance of including direct reactions in deuteron-induced nucleon-emission calculations is confirmed, and use of a simple Serber model is shown to give good agreement with data. Finally, the importance of multiple preequilibrium effects in calculations of (n,2nγ) and (n,3nγ) reactions is demonstrated, together with the applicability of the model used in the GNASH code.

5. Acknowledgments

We would like to thank Prof. H. Vonach, Dr. R. Haight, and their co-workers for use of their experimental results prior to final publication.

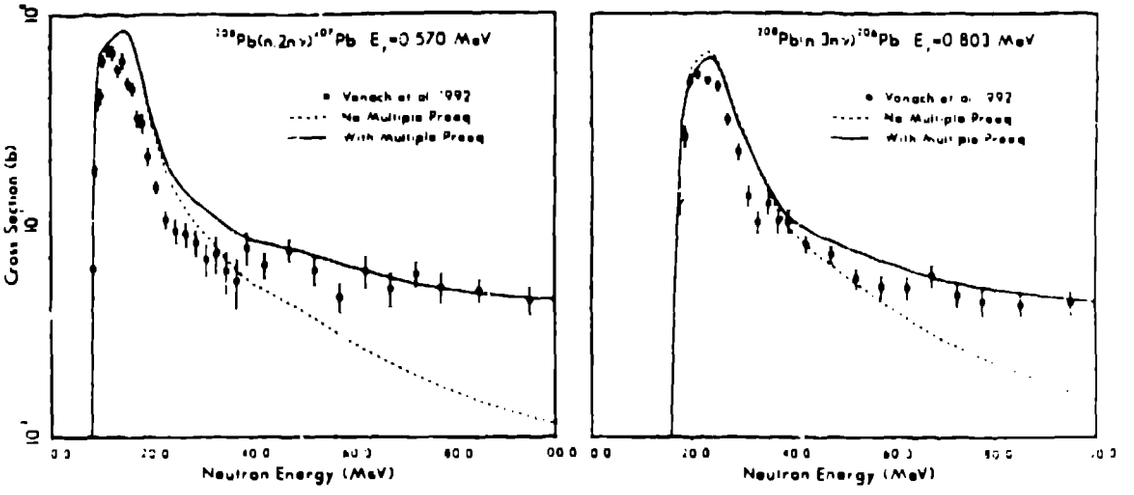

Fig. 8. Comparison of $^{208}Pb(n,2n\gamma)^{207}Pb$ and $^{208}Pb(n,3n\gamma)^{206}Pb$ cross sections calculated with and without multiple preequilibrium effects with the data of Vonach et al.[10]

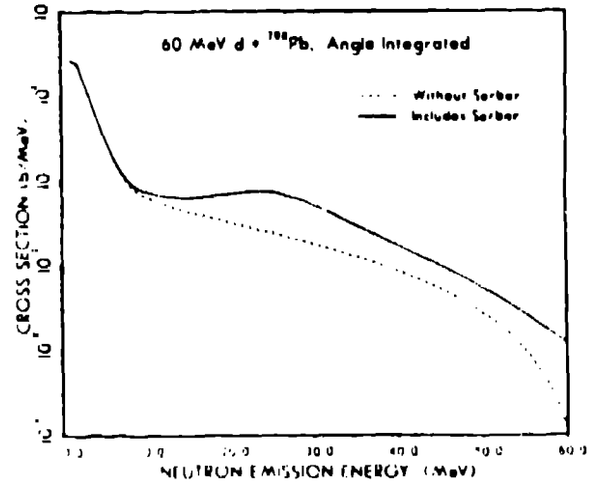

Fig. 9. Calculated neutron emission spectra from 60-MeV d + ^{208}Pb reactions with and without direct components from a Serber model.[22]

6. References

1. P.G. Young and E.D. Arthur, "GNASH: A Preequilibrium, Statistical Nuclear Model Code for Calculation of Cross Sections and Emission Spectra," LA-6947 (1977).

2. N.Yamamuro, "Nuclear Cross Section Calculations with a Simplified-Input Version of ELIESE-GNASH Joint Program," Proc. Int. Conf. on *Nucl. Data for Sci. and Tech.*, Mito (1988) p.489, and JAERI-M 90-006 (1990).

3. E.D. Arthur, "The GNASH Preequilibrium Statistical Model Code," Proc. ICTP Wksp. on *Applied Nucl. Theory and Nucl. Model Calculations for Nucl.Tech. Applications*, 15 Feb. - 18 Mar., 1988, Trieste, Italy.

4. P.G. Young, E.D. Arthur, and M.B. Chadwick, "Comprehensive Nuclear Model Calculations: Introduction to the Theory and Use of the GNASH Code," Proc. ICTP Workshop on *Comp. and Anal. of Nucl. Data Relevant to Nucl. En. and Safety*, 10 Feb. - 13 Mar., 1992, Trieste, Italy, and LA-12343-MS (1992).

5. E.D. Arthur and P.G. Young, "Evaluation of Neutron Cross Sections to 40 MeV for ^{54,56}Fe," Proc. Sym. on *Neutron Cross Sections from 10 to 50 MeV*, Brookhaven National Laboratory, Upton, N.Y., 12-14 May 1980, BNL-NCS-51245 (1980)] v. II, p. 731, and LA-8626-MS (1980).

6. E.D. Arthur, P.G. Young, and W.K. Matthes, "Calculation of ^{59}Co Neutron Cross Sections between 3 and 50 MeV," Proc. Sym. on *Neutron Cross Sections from 10 to 50 MeV*, Brookhaven National Laboratory, Upton, N.Y., 12-14 May 1980, BNL-NCS-51245 (1980)] v. II, p. 751.

7. P. G. Young, R. C. Haight, R. O. Nelson, S. A. Wender, C. M. Laymon, G. L. Morgan, D. M. Drake, M. Drosg, H. Vonach, A. Pavlik, S. Tagesen, D. C. Larson, and D. S. Dale, "Calculation of (n,xγ) Cross Sections between Threshold and 100 MeV for Fe and Pb Isotopes: Comparisons with Experimental Data," IAEA CRP Meeting on *Methods for the Calculation of Neutron Nuclear Data for Structural Materials of Fast and Fusion Reactors*, Vienna, Austria, 20-22 June 1990, INDC(NDS)-247 (1991) p. 239.

8. P. G. Young, E. D. Arthur, M. Bozoian, T. R. England, G. M. Hale, R. J. LaBauve, R. C. Little, R. E. MacFarlane, D. G. Madland, R. T. Perry, and W. B. Wilson,*Trans. Amer. Nucl. Soc.* **60**, 271 (1989), and LA-11753-MS (1990).

9. A. Gilbert and A. G. W. Cameron, *Can. J. Phys.* **43**, 1446 (1965).

10. A. V. Ignatyuk, G. N. Smirenkin, and A. S. Tishin, *Sov. J. Nucl. Phys.* **21**, 255 (1975).

11. C. Kalbach, *Z. Phys. A* **283**, 401 (1977).

12. C. Kalbach,*Phys. Rev. C* **37**, 2350 (1988); see also C. Kalbach and F. M. Mann, *Phys. Rev. C* **23**, 112 (1981).

13. D.G. Madland, "A Preliminary Medium-Energy Nucleon-Nucleus Phenomenological Optical Model Potential," Proc. IAEA Advisory Group on *Nuclear Theory for Fast Neutron Data Evaluation*, Beijing, Peoples Republic of China, 12-16 Oct. 1987, IAEA-TECDOC-483 (1988) p.80.

14. For example, D. Wilmore and P.E. Hodgson, *Nucl. Phys.* **55**, 673 (1964); F. D. Becchetti, Jr., and G. W. Greenlees, *Phys. Rev.* **182**, 1190 (1969).

15. P.W. Lisowski, C.F. Auchampaugh, M.S. Moore, G.L. Morgan, and R.E. Shamu, "Neutron Cross Section Measurements at WNR," Proc. Sym. on *Neutron Cross Sections from 10 to 50 MeV*, 12-14 May 1980, Brookhaven National Laboratory, BNL-NCS-51245 (1980) p. 301.

16. R.L. Schutt, R.E. Shamu, P.W. Lisowski, M.S. Moore, and G.L. Morgan, *Phys. Le.t. B* **203**, 22 (1988).

17. R. W. Finlay, J. R.M. Annand, T. S. Cheema, and J. Rapaport, *Phys. Rev. C* **30**, 796 (1984).

18. P.G. Young and R.E. Shamu, Proc. Sym. on *Nuclear Data Evaluation Methodology*, 12-16 October 1992, Brookhaven National Laboratory, to be issued.

19. H. Vonach and R. Haight, personal communication; see also R. C. Haight, D.M. Drake, M. Drosg, C.M. Laymon, G.L. Morgan, R.O. Nelson, S.A. Wender, P.G. Young, H. Vonach, A. Pavlik, S. Tagesen, D.C. Larson, and D.S. Dale, *Bull. Am. Phys. Soc.* **35**, 1038 (1990).

20. J. Martin, R. Kiziah, D. Ek, N. Miller, B. Johnston, D. Rutherford, and W. Wilson, "Neutron and Gamma-Ray Production from Range Thick Targets Bombarded with 98-MeV Deuterons," Air Force Weapons Laboratory, Albuquerque, NM, personal communication (1988).

21. D. C. Larson, "High-Resolution Structural Material (n,xγ) Production Cross Sections for $0.2 < E_n \leq 40$ MeV," Proc. Int. Conf. on *Nuclear Data for Basic and Applied Science*, May 13-17, 1985, Santa Fe, N. M. (Ed. P.G. Young, R.E. Brown, G.F. Auchampaugh, P.W. Lisowski, and L. Stewart, Gordon and Breach, New York,1986) V. 1, p. 71.

22. W. Dilg, W. Schantl, H. Vonach, and M. Uhl, *Nucl. Phys.* **A217**, 269 (1973).

23. R. Serber, *Phys. Rev.* **72**, 1008 (1947).